The Journal of Prevention of Alzheimer's Disease 12 (2025) 100323

Contents lists available at ScienceDirect

The Journal of Prevention of Alzheimer's Disease

journal homepage: www.elsevier.com/locate/tjpad

A novel early imaging biomarker for glymphatic function: Cerebral cortical arterial pulsatility index from 2-Minute phase-contrast MRI

Sung-Hye You [a], Byungjun Kim [a,*], Moonjung Hwang [a], Kyung-Sook Yang [b], Hye-Won Park [a], InSeong Kim [c], SuGil Kim [c], Kyung Min Kim [a], Bo Kyu Kim [a], Jae Ho Shin [a]

[a] Department of Radiology, Anam Hospital, Korea University College of Medicine, 73, Goryeodae-ro, Seongbuk-gu, Seoul 02841, Republic of Korea
[b] Department of Biostatistics, Korea University College of Medicine, Republic of Korea
[c] Siemens Healthineers, Republic of Korea

ARTICLE INFO

Keywords:
2D Phase-contrast MRI
Pulsatility index
Glymphatics
Alzheimer's disease

ABSTRACT

Background: Arterial pulsatility is one of the driving forces of glymphatic flow.
Objectives: To evaluate the feasibility of the pulsatility index (PI) of cortical arteries in the centrum semiovale (PI_{CSO}) as a novel non-invasive imaging biomarker for Alzheimer's disease (AD) in the context of glymphatic function.
Design: Retrospective cross-sectional study.
Setting: Single tertiary academic center equipped with both 3.0 T MRI systems.
Participants: A total of 160 individuals were enrolled: 50 healthy volunteers, 46 cognitively normal controls, and 64 AD patients who underwent diffusion tensor imaging (DTI) and 2D phase-contrast MRI.
Measurements: Diffusion Tensor Imaging Analysis along the Perivascular Space (DTI-ALPS) index and PI_{CSO} were assessed using 2D phase-contrast MRI. Correlations with age, DTI-ALPS index, and Mini-Mental State Examination (MMSE) scores were analyzed.
Results: PI_{CSO} was significantly higher in the AD group than those in healthy volunteers ($P<0.001$) and cognitively normal aging ($P=0.001$) groups. PI_{CSO} correlated positively with age (rho=0.613, $P<0.001$) and negatively with both the DTI-ALPS index (rho=-0.439, $P<0.001$) and MMSE scores (rho=-0.486, $P<0.001$) in total group.
Conclusion: PI_{CSO} derived from 2D phase-contrast 3.0T MRI may serve as a novel imaging biomarker for Alzheimer's disease in relation to glymphatic function.

Abbreviations

AD	Alzheimer's disease
CDR-SB	clinical dementia rating sum of boxes
CSO	centrum semiovale
DTI-ALPS	diffusion tensor image analysis along the perivascular space
MMSE	Mini-Mental State Examination
PI	pulsatility index
PI_{CSO}	pulsatility index of cortical artery in centrum semiovale level
SNSB-II	Seoul Neuropsychological Screening Battery-II
PC-MRI	phase-contrast magnetic resonance imaging

1. Introduction

Over the past two decades, several studies have proposed that cerebral small vessel pathologies may negatively impact on cognitive function [1–4], and related imaging parameters have attracted attention as early imaging biomarkers of neurodegeneration [5–7]. Recently, several studies have demonstrated a correlation between cerebral arterial wall stiffness and cognitive impairment [5,8–10]. Although the exact underlying mechanism remains unclear, one plausible explanation is that the pulsation of small perforating arteries plays a crucial role as a driving force for glymphatic flow [4,5,11,12]. Reduced clearance of amyloid-beta due to impaired glymphatic flow resulting from vascular stiffness may increase the risk of Alzheimer's disease (AD) [11].

While MRI following intrathecal contrast administration or serial

* Corresponding author.
E-mail address: bj1492.kim@gmail.com (B. Kim).

https://doi.org/10.1016/j.tjpad.2025.100323
Received 11 June 2025; Received in revised form 22 July 2025; Accepted 3 August 2025
Available online 14 August 2025

imaging after intravenous contrast injection represents the most accurate method for assessing glymphatic function, the inherent invasiveness of these approaches has spurred increasing interest in the development of non-invasive MR-based alternatives. To date, the Diffusion Tensor Image Analysis along the Perivascular Space (DTI-ALPS) index, which reflects perivascular glymphatic flow, has been the most thoroughly investigated and has shown potential as an indirect imaging biomarker for estimating glymphatic function [13,14]. In addition, several other advanced imaging sequences have been explored, targeting various aspects of the glymphatic system, including cerebrospinal fluid (CSF) flow, CSF production, aquaporin-4 (AQP4) channel activity, and meningeal lymphatic vessels [13–17]. However, studies on glymphatic function in relation to arterial pulsation are limited. Phase-contrast magnetic resonance imaging (PC-MRI) is a widely used technique that measures flow velocity by detecting phase shifts induced by bipolar gradients [6]. The pulsatility index (PI), derived from blood flow curves, serves as an indirect indicator of vascular wall stiffness [7,18,19]. Thus, PI can theoretically be considered a glymphatic parameter in terms of the vascular driving force for glymphatic flow. Since impaired pulsatility may hinder glymphatic clearance, a lower PI could be associated with increased risk for Alzheimer's disease and may therefore be hypothesized to be lower in the AD group.

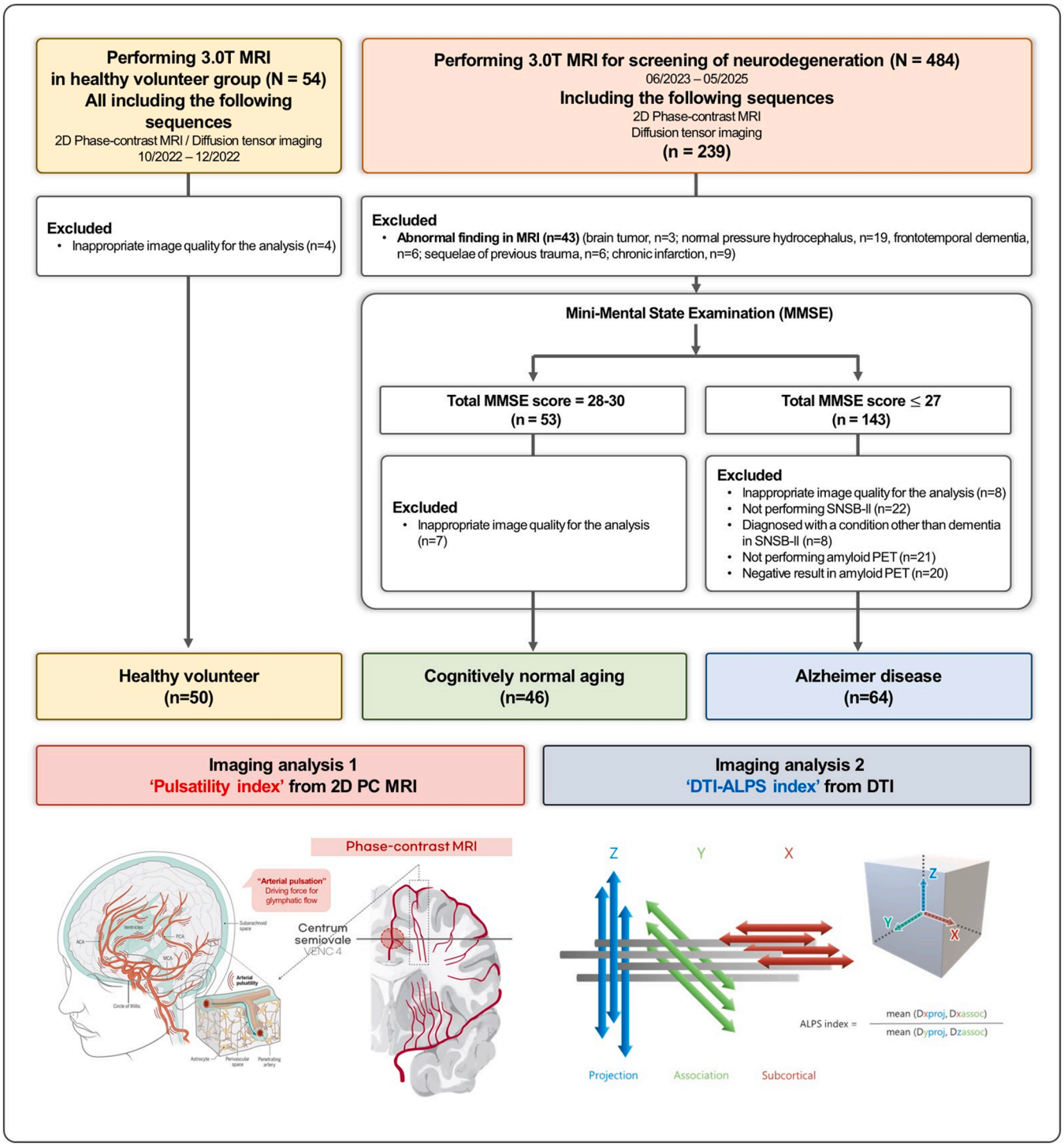

Fig. 1. Study design. Note: SNSB-II = Seoul Neuropsychological Screening Battery-II.

Nevertheless, owing to technical challenges in measuring phase shifts in small cerebral arteries, most previous PC-MRI studies on these vessels have been conducted using 7.0 T MRI [20–28]. These studies have established correlations between PI and factors such as age, intracerebral hemorrhage, hypertension, and number of perivascular spaces [21–24,27]. Given the limited accessibility of 7.0 T MRI in routine clinical practice, a few studies attempted to apply PC-MRI for cerebral arteries using 3.0 T MRI [29,30]. One study performed 3.0 T PC-MRI on the proximal internal carotid artery to reveal its correlation with cognitive impairment [5], while recent studies have explored the feasibility of using 3.0 T MRI to obtain the PI in perforating arteries within the centrum semiovale (CSO) and basal ganglia (BG) [29,30].

In addition to demonstrating the feasibility of measuring the PI of cortical arteries using 3.0 T PC-MRI, the potential association between PI and AD, particularly in the context of glymphatic function, has not yet been investigated. Therefore, this study aimed to evaluate whether the PI of cortical arteries at the centrum semiovale level (PI_{CSO}), derived from 3.0 T MRI, could serve as a novel, non-invasive imaging biomarker for AD in relation to glymphatic function.

2. Methods

2.1. Patient selection 1: healthy volunteer (HV) group

This prospective, single-center study was approved by the institutional review board of Korea University Anam Hospital, and informed consent was obtained from all participants. From October 2022 to December 2022, 54 healthy volunteers were enrolled and underwent 3.0 T MRI using the Magnetom Vida (Siemens Healthineers, Erlangen, Germany) (Fig. 1). The imaging protocol included three-dimensional (3D) T1-weighted imaging (T1WI), PC-MRI, and diffusion tensor imaging (DTI) sequences. Four participants were excluded due to inadequate image quality for analysis. Demographic and clinical data, including age, sex, and Mini-Mental State Examination (MMSE) scores, were collected.

2.2. Patient selection 2: Neurodegeneration screening group

This single-center, retrospective study was approved by the institutional review board of the same institution, and the requirement for informed consent was waived because of the retrospective nature of this study. From June 2023 to May 2025, a total of 484 participants underwent 3.0T brain MRI as part of a neurodegeneration screening protocol, and 239 individuals who performing both DTI and 2D PC-MRI were eligible for further analysis (Fig. 1). Among them, forty-three participants were excluded due to abnormal MRI findings, including brain tumor (n = 3), normal pressure hydrocephalus (n = 19), frontotemporal dementia (n = 6), sequelae of previous trauma (n = 6), and chronic infarction (n = 9). The remaining participants (n = 196) were classified into two groups: cognitively normal aging (MMSE 28–30, n = 53) and suspected cognitive impairment (MMSE $\leq$ 27, n = 143). In the cognitively normal (CN) group, seven participants were excluded due to inadequate image quality, resulting in 46 subjects for final analysis. In the suspected cognitive impairment group, 79 participants were excluded for the following reasons: inadequate image quality (n = 8), no completion of Seoul Neuropsychological Screening Battery-II (SNSB-II) (n = 22), diagnosed with a condition other than dementia in SNSB-II (n=8), absence of amyloid PET imaging (n = 21), or negative amyloid PET results (n = 20). Ultimately, 64 participants with positive amyloid PET findings and consistent SNSB-II results were classified as having Alzheimer's disease based on the diagnostic criteria for AD as defined by the 2011 National Institute on Aging–Alzheimer's Association (NIA-AA) guidelines [31]. The following clinical information related to cognitive impairment was collected: age, sex, MMSE score, APOE4 genotyping results, years of education, presence of hypertension or type 2 diabetes, and SNSB-II results.

2.3. Imaging acquisition

MRI was performed with 3.0 T MRI scanners (Magnetom Vida, Prisma_fit, Magnetom Skyra [Siemens Healthineers, Erlangen, Germany]; Signa Premier [GE Healthcare, Milwaukee, WI, USA]; Ingenia Elition X [Philips Healthcare, Best, Netherlands]) with 64-channel head coils. The specific MRI parameters of DTI and PC-MRI sequences are listed in Supplementary Table 1. A peripheral pulse oximeter was used for cardiac gating. The target slice for PI_{CSO} was positioned 15 mm above the upper margin of the corpus callosum body.

2.4. Imaging analysis

Glymphatic function was assessed using two main indices: the DTI-ALPS index for perivascular glymphatic flow and PI for the driving force of glymphatic flow (Fig. 2). The DTI-ALPS index was calculated using DTI data, while the PI was derived from 2D PC-MRI.

2.5. Parameter for perivascular glymphatic flow: DTI-ALPS index

The DTI-ALPS index, which reflects perivascular glymphatic flow, was measured under the hypothesis that it may be reduced in AD. The DTI-ALPS index was calculated using the following formula proposed by Taoka et al. (Fig. 2):

$$DTI - ALPS\ index = \frac{mean\left(Dxx_{proj},\ Dxx_{assoc}\right)}{mean\left(Dyy_{proj},\ Dzz_{assoc}\right)}$$

Three preprocessing steps were performed before calculating the DTI-ALPS index. For perivascular glymphatic flow, the DTI-ALPS index was used. The analysis began with preprocessing of the DTI data using MRTrix3. This preprocessing included denoising, unringing, and eddy current correction to enhance the quality of the diffusion data. Next, the preprocessed data were fitted using the FMRIB Software Library to create diffusion maps, specifically, the Dxx, Dyy, and Dzz maps, which represent the diffusion coefficients along the x-, y-, and z-axes, respectively. These steps were performed on individual datasets. Following fitting, fractional anisotropy (FA) maps were normalized using a template (JHU-ICBM-FA-1 mm.nii.gz) through both linear and non-linear registration processes, ensuring that the diffusion data were aligned to a common space for accurate comparison. Regions of interest (ROIs) were then extracted based on specific anatomical landmarks. The DTI-ALPS index was calculated by measuring the mean diffusivity along the projection and association fibers. The ALPS index was determined as the ratio of the mean (Dxproj, Dyassoc) to mean (Dzassoc). The resulting ALPS index values from the right and left hemispheres were averaged to obtain a mean value for each participant.

2.6. Parameter for arterial wall stiffness: pulsatility index

The PI, reflecting arterial wall stiffness, was calculated as a potential imaging biomarker of glymphatic function, representing the driving force of CSF flow into the brain interstitial space, under the hypothesis that it may be elevated in AD. The PI_{CSO} was derived from PC-MRI data using Circle Cardiovascular Imaging software (Fig. 2). The PI was calculated using the following formula based on the flow velocity curve: Pulsatility Index (PI) = $|\frac{Vmax - Vmin}{Vmean}|$, where V_{max} is the maximum velocity, V_{min} is the minimum velocity, and V_{mean} is the mean velocity of blood flow. The ROIs were placed on four cortical arteries—distal branches of the anterior cerebral artery—at the CSO level (PI_{CSO} 1: right medial frontal area; PI_{CSO} 2: left medial frontal area; PI_{CSO} 3: right medial parietal area; PI_{CSO} 4: left medial parietal area) to identify the artery coursing most orthogonally to the axial imaging plane at this level. Four ROIs were manually placed on the magnitude images showing the highest signal intensity with a round shape, and the mean

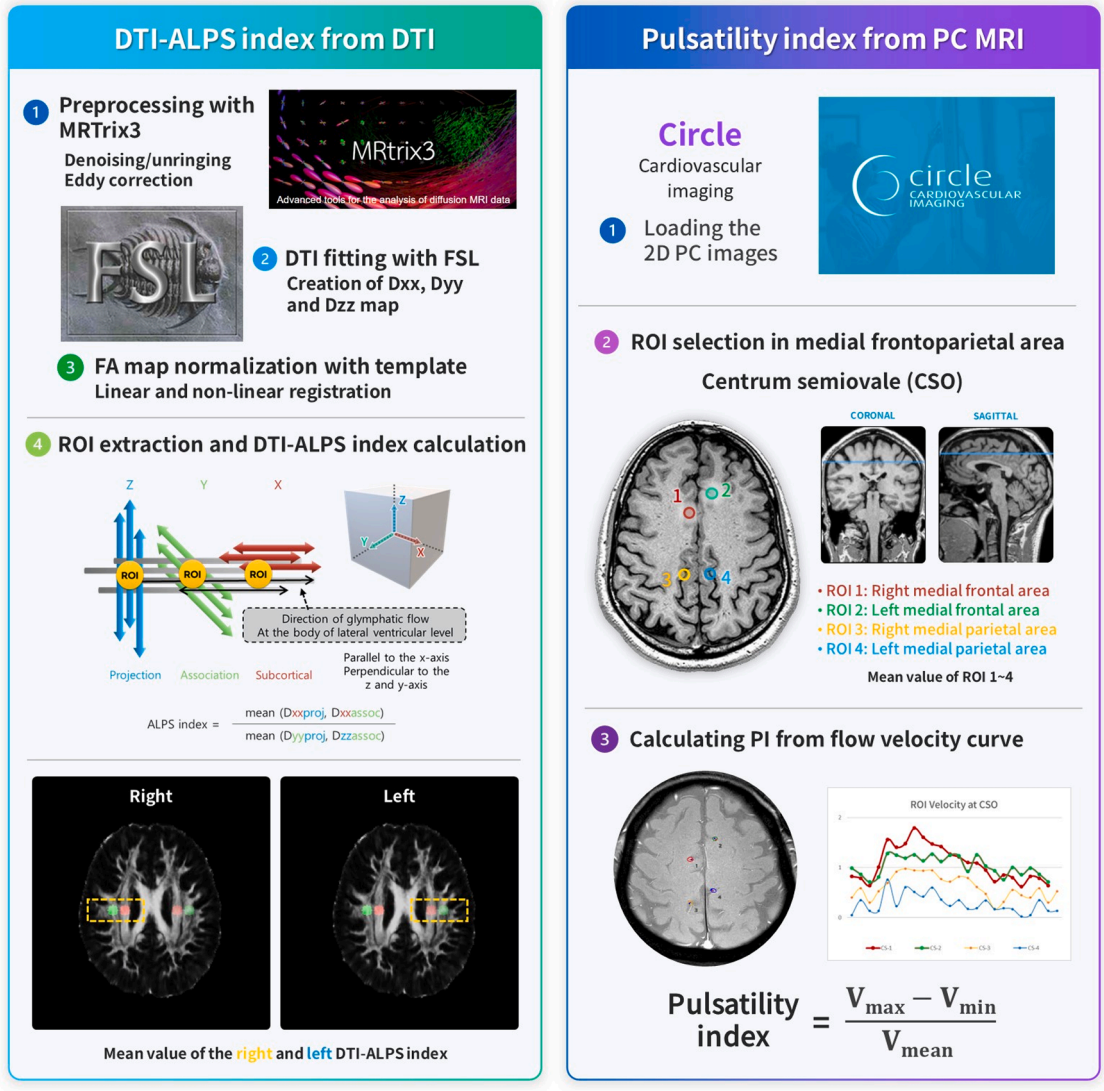

Fig. 2. Measurement of Diffusion Tensor Image Analysis along the Perivascular Space (DTI-ALPS) index and pulsatility index (PI).

PI_{CSO} was calculated from the values of four ROIs.

2.7. Statistical analysis

Statistical analyses were performed using MedCalc version 19.5.3 (MedCalc Software, Mariakerke, Belgium). Continuous variables were tested for normality using the Shapiro–Wilk test and were found to have non-normal distributions; hence, they were presented as median and interquartile range (IQR). Categorical variables were expressed as frequencies and percentages. Group comparisons among HV, CN, and AD groups were conducted using the Kruskal–Wallis H test for continuous variables and the chi-square test for categorical variables. For post-hoc analyses of continuous variables, Dunn's test was applied to assess pairwise differences between groups. A P value less than 0.05 was considered statistically significant. The reliability of PI_{CSO} measurements data was evaluated using the intraclass correlation coefficient among the four ROIs. Spearman's rank correlation coefficient (rho) was used to evaluate the associations between the PI_{CSO}, age, MMSE scores, and the DTI-ALPS index. Correlation analyses were performed in the overall cohort and within each diagnostic subgroup (HV, CN, and AD). Ninety-five percent confidence intervals (95% CI) were calculated for correlation coefficients.

3. Results

3.1. Patients

The baseline characteristics of the HV, CN, and AD groups are presented in Table 1. A total of 160 participants were included in the final analysis: 50 HV, 46 CN, and 64 patients with AD. There was a significant difference in age across the groups ($P < 0.001$), with HV being significantly younger than both CN and AD groups (both $P < 0.001$), while no significant difference was observed between CN and AD ($P = 0.980$). MMSE scores were significantly lower in the AD group compared to both HV and CN groups (both $P < 0.001$).

3.2. Comparison of DTI-ALPS index and PI_{CSO} among the three groups

As presented in Supplementary Table 2 and Fig. 3, there were significant differences in both the DTI-ALPS index and PI_{CSO} among the three groups (both $P < 0.001$). The DTI-ALPS index was highest in HV (median [IQR], 1.392 [1.350;1.429]), followed by CN (median [IQR], 1.305 [1.270;1.380]), and lowest in the AD group (1.280 [1.215;1.330]). Post-hoc analysis revealed that the AD group showed significantly lower DTI-ALPS values compared to both HV ($P < 0.001$) and CN ($P = 0.026$). Conversely, PI_{CSO} was significantly elevated in the

Table 1
Patient characteristics.

	Healthy volunteer (HV) (n = 50)	Cognitively normal aging (CN) (n = 46)	Alzheimer's disease (AD) (n = 64)	P value	HV vs. CN[b]	HV vs. AD[b]	CN vs. AD[b]
Age[a,b]	43.000 [34.000;55.000]	78.000 [68.000;83.000]	80.000 [73.000;83.000]	<0.001[d]	<0.001	<0.001	0.980
Sex, female[c]	26 (52.000%)	27 (58.696%)	41 (64.062%)	0.431[d]			
MMSE, total score[a,b]	29.000 [29.000;30.000]	28.000 [28.000;30.000]	25.000 [22.000;27.000]	<0.001[d]	0.126	<0.001	<0.001
APOE4 status (No. of ε4)[c]				0.248[e]			
NA	50 (100.000%)						
0	NA	33 (71.739%)	39 (60.938%)				
1	NA	11 (23.913%)	23 (35.938%)				
2	NA	2 (4.348%)	1 (1.562%)				
Education (y)[a]	NA	12.000 [8.000;16.000]	9.000 [6.000;15.000]	0.049[e]			
Hypertension[a,c]	NA	26 (56.522%)	29 (45.312%)	0.248[e]			
Type 2 diabetes mellitus[a,c]	NA	16 (34.783%)	22 (34.375%)	0.864[e]			
Neuropsychologic assessment (SNSB-II)							
CDR-SB[a]	NA	NA	1.500 [0.500;3.000]				
SGDS[a]	NA	NA	4.000 [1.500;8.000]				
Barthel-ADL[a]	NA	NA	20.000 [20.000;20.000]				
GDS[a]	NA	NA	3.000 [3.000;4.000]				

Note. MMSE = Mini-Mental State Examination; APOE4 = apolipoprotein E ε4 allele; SNSB-II = Seoul Neuropsychological Screening Battery-II; CDR-SB = Clinical dementia Rating Sum of Boxes; SGDS = Short Version of the Geriatric Depression Scale; Barthel-ADL = Barthel-Activities of Daily Living; GDS = Global Deterioration Scale

[a] Data are presented as median [interquartile range] owing to their non-normal distribution.
[b] Group comparisons were performed using the Kruskal-Wallis H test, followed by Dunn's post-hoc test as a post-hoc analysis
[c] Chi-square test
[d] P value among the three groups
[e] P value between the second and third groups

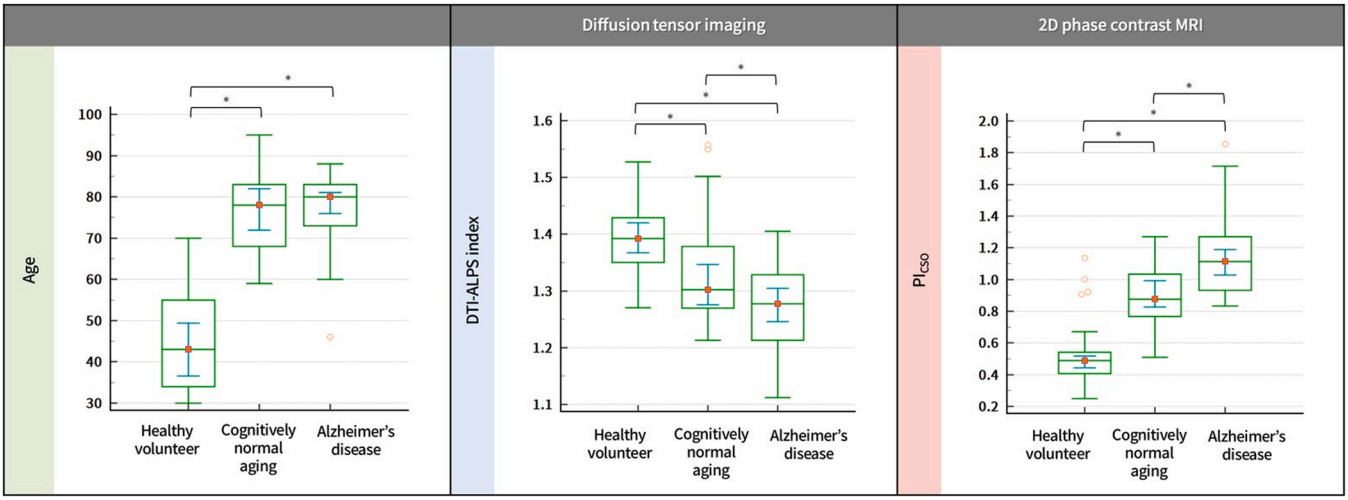

Fig. 3. Comparison of Diffusion Tensor Image Analysis along the Perivascular Space (DTI-ALPS) index and pulsatility index (PI) among the healthy volunteers, cognitively normal, and Alzheimer's disease groups. Note: In this box-and-Whisker plot, the green box represents the interquartile range (IQR), the horizontal line inside the box indicates the median, the red square shows the mean, and the blue bars denote the 95% confidence interval of the mean. Whiskers extend to the minimum and maximum values within 1.5×IQR, and orange circles indicate outliers. *indicates P < 0.05.

AD group (median [IQR], 1.115 [0.930;1.270]) compared to CN (median [IQR], 0.875 [0.770;1.030], P = 0.001) and HV (median [IQR], 0.490 [0.410;0.540], P < 0.001). Regarding the reliability of PI_{CSO}, the intraclass correlation coefficient among the 4 ROIs was 0.786 (95% CI, 0.726 to 0.835).

3.3. Correlation of PI_{CSO} with age, MMSE score, and DTI-ALPS index

Supplementary Table 3 and Fig. 4 shows the correlation between PI_{CSO} with age, MMSE score, and DTI-ALPS index. In the total cohort (N = 160), PI_{CSO} showed a positive correlation with age (rho = 0.613, P < 0.001), and negative correlations with MMSE score (rho = –0.486, P < 0.001) and DTI-ALPS index (rho = –0.439, P < 0.001). In the non-AD group (HV + CN; n = 96), PI_{CSO} was significantly correlated with age (ρ = 0.575, 95% CI: 0.423–0.695, P < 0.001), negatively correlated with MMSE score (ρ = –0.273, 95% CI: –0.449 to –0.076, P = 0.007), and with DTI-ALPS index (ρ = –0.319, 95% CI: –0.488 to –0.126, P = 0.002). In the AD group (n = 64), no significant correlations were observed

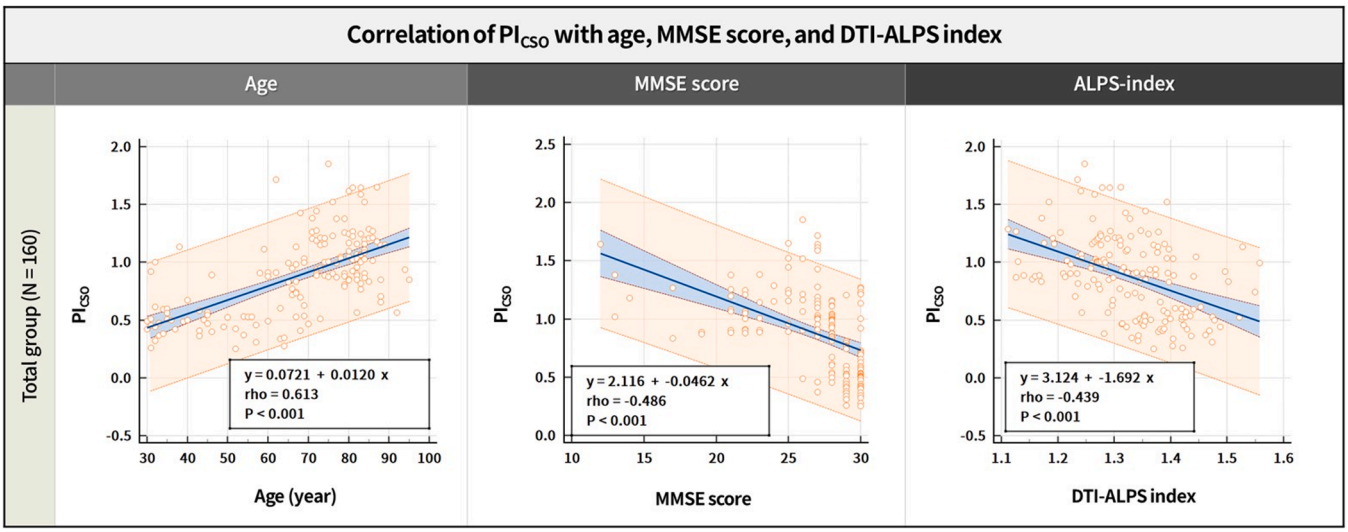

Fig. 4. Correlation of pulsatility index (PI) with age, Mini-Mental State Examination (MMSE) score, and Diffusion Tensor Image Analysis along the Perivascular Space (DTI-ALPS) index. Note: Each dot represents an individual participant. The solid blue line indicates the linear regression fit, with shaded areas representing the 95% confidence interval. The dashed orange lines indicate the 95% prediction interval. Linear regression equations, Spearman's correlation coefficients (rho), and P-values are provided in each panel.

between PICSO and age ($\rho = 0.094$, $P = 0.462$), MMSE score ($\rho = 0.067$, $P = 0.597$), or DTI-ALPS index ($\rho = 0.067$, $P = 0.601$).

4. Discussion

The key findings of our study are as follows: (1) PI_{CSO} was significantly higher in the AD group compared to CN and HV groups. (2) PI_{CSO} exhibited a positive correlation with age and a negative correlation with both the DTI-ALPS index and MMSE scores.

4.1. PI_{CSO}, glymphatic function, and AD

In our study, PI_{CSO} was significantly higher in the AD group. Additionally, it was negatively correlated with the DTI-ALPS index and MMSE score. One potential mechanism underlying the correlation between elevated PI_{CSO} and AD is that increased vascular wall stiffness reduces the pulsatile force driving glymphatic flow, leading to the accumulation of cerebral metabolic waste products, such as amyloid-beta, which in turn contributes to AD. Concurrently, amyloid-beta deposition within the perivascular space may increase vascular stiffness, creating a vicious cycle that exacerbates vascular wall damage and stiffening. The DTI-ALPS index has been established as a glymphatic biomarker in previous studies. The positive correlation observed between the DTI-ALPS index and PI_{CSO} suggests that this new index may serve as a novel, non-invasive imaging biomarker for Alzheimer's disease in the context of glymphatic dysfunction. Furthermore, in the future, PI_{CSO} might serve as a potential monitoring marker for treatments targeting amyloid-beta, such as monoclonal antibody therapies like lecanemab, as perivascular amyloid-beta deposition could increase vascular stiffness.

4.2. PI_{CSO} and endothelial dysfunction

Elevated PI_{CSO} may also be linked to endothelial dysfunction, a pathological process that contributes to cognitive decline via vascular dementia-related mechanisms [21,32]. In younger individuals, cerebral small arteries maintain proper endothelial function and vascular compliance, effectively dampening the transmission of cardiac pulsation from the aortic artery [26,33]. This compensation reduces the exposure of small cerebral vessels to hemodynamic stress and endothelial damage [26]. However, with aging and the accumulation of cardiovascular risk factors, such as hypertension, endothelial dysfunction and vascular stiffness progressively develop [24]. Loss of smooth muscle cells, endothelial damage, lipohyalinosis, and fibrinoid necrosis contribute to functional abnormalities and mechanical stiffening of the arterial wall through increased collagen fiber synthesis. Thus, cerebrovascular flow imaging has the potential to serve as an early biomarker for detecting small vessel dysfunction before more advanced parenchymal changes, such as white matter hyperintensity or brain atrophy, become apparent.

4.3. Comparison of PI in 3.0 T vs. 7.0 T MRI

The degree of phase-shifting in MRI is influenced by gradient performance [6]. As a result, most previous studies using PC-MRI for small cerebral arteries were conducted using 7.0 T MRI [23]. However, given that ultra-high-field MRI is primarily limited to research settings, evaluating the feasibility of 3.0 T MRI is crucial for broader clinical applications. Although the vascular detection sensitivity of 3.0 T MRI is approximately five times lower than that of 7.0 T MRI for phase-contrast imaging [19], a previous study demonstrated that PI measurements are feasible at 3.0 T [29]. In that study, no direct correlation between 3.0 T and 7.0 T MRI in terms of flow velocity and PI values was established because 3.0 T MRI is only capable of detecting relatively larger arteries. Consistent with previous research, our study also identified the feasibility of PI measurement in 3.0T MRI. Considering accessibility, measuring PI using 3.0 T MRI showed potential as a good alternative to 7.0 T MRI.

4.4. Cortical artery vs. perforating artery as a target vessel

In our study, we selected cortical arteries at the CSO level rather than perforating arteries for two reasons: [1] the manual detection of perforating arteries in 3.0 T MRI was expected to have low reliability due to poor signal intensity, and [2] PI values reflect not only the compliance of the targeted vessel but also that of downstream smaller vascular structures [5,25,33]. Fortunately, PI_{CSO} from cortical vessels correlated well with the DTI-ALPS index and MMSE scores in 3.0 T MRI. This suggests that cortical artery-based PI measurement in 3.0 T MRI may be feasible alternative to perforating artery-based measurements in 7.0 T MRI.

4.5. PI Measurement Using 2D vs. 4D PC-MRI

Recent studies have explored the use of 4D PC-MRI for PI calculation across multiple intracranial arteries [33,34]. This technique offers several advantages, such as the ability to assess any desired artery and measure additional parameters, including the damping index and pulse wave velocity [6,33,34]. However, 4D PC-MRI requires a scan time of approximately 10 min and involves complex post-processing [5,6,33]. Furthermore, its application is limited to selected MRI scanners, and a critical drawback is its reduced feasibility for assessing small vessels owing to its low spatial resolution and high VENC values required for covering a diverse range of arteries [5,6]. In contrast, 2D PC-MRI is available on all commercial MRI scanners, has a significantly shorter scan time (approximately 2–3 min), and requires simpler post-processing. Given these advantages, 2D PC-MRI at the CSO level may be more suitable than whole-brain 4D PC-MRI for evaluating glymphatic function.

4.6. Limitations

This study had several limitations. **First,** it was a single-center study with a relatively small sample size. Future prospective multicenter studies with larger cohorts are required to validate our findings. **Second,** we could not evaluate the correlation of PI_{CSO} with other more comprehensive and accurate methods to reflect glymphatic function such as MRI after intrathecal contrast injection or repeated MRI after intravenous contrast injection due to its invasiveness and inconvenience of the patients. Although the usefulness of DTI-ALPS index is evaluated in many previous studies and the most widely applied to evaluate the perivascular glymphatic flow due to its non-invasiveness and convenience, further animal study or using repeated MRI is warranted to obtain more firm evidence for this new parameter. **Third,** given that amyloid PET-CT was not performed in the HV and CN groups, the possibility of including participants with subclinical Alzheimer's disease cannot be excluded. As our institution does not routinely perform amyloid PET-CT in individuals without clinical evidence of cognitive impairment, direct comparison was not feasible. Further prospective studies involving amyloid PET-CT in these populations are warranted. **Fourth**, we selected four cortical arteries at the CSO level rather than performing whole-artery segmentation. A previous study reported that single round-shaped artery selection is more accurate than whole-artery segmentation because data from obliquely scanned arteries are inaccurate in 2D PC-MRI [28]. Thus, we manually selected the most round-shaped high-signal-intensity vessel. This method is intuitive, does not require a special post-processing algorithm, and showed good agreement among the four vessels in terms of PI values. However, further study is required to compare the accuracy between four-vessel selection and whole-vessel segmentation methods. **Fifth,** in the non-AD group, two distinct participant profiles were present. The HV group tended to be significantly younger, as participants were recruited based on their eligibility to undergo simultaneous 7.0T MRI, in order to conduct a preliminary assessment of the feasibility of 2D phase-contrast MRI at 3.0T. In contrast, the CN group included relatively older individuals, reflecting the nature of their recruitment for neurodegeneration evaluation. This heterogeneity across groups may introduce ambiguity in the interpretation of the study findings. Therefore, future comparative studies should include a more representative control group, such as individuals undergoing brain MRI as part of routine health screening.

5. Conclusion

PI_{CSO}, derived from 2D phase-contrast imaging in 3.0 T MRI, shows promise as a potential non-invasive imaging biomarker for AD in the context of glymphatic function.

Funding

- This work was supported by the National Research Foundation of Korea (NRF) grant funded by the Korea government (MSIT, Ministry of Science and ICT) (Grant No. RS-2023-00209819)
- This research was supported by a grant of the Korea Health Technology R&D Project through the Korea Health Industry Development Institute (KHIDI), funded by the Ministry of Health & Welfare, Republic of Korea (grant number: RS-2022-KH129293)
- This work was supported by the Korea Medical Device Development Fund grant funded by the Korea government (the Ministry of Science and ICT, the Ministry of Trade, Industry and Energy, the Ministry of Health & Welfare, the Ministry of Food and Drug Safety) (Project Number: 1711138003, Grant No. RS-2020-KD000041)

The sponsors had no role in the design and conduct of the study; in the collection, analysis, and interpretation of data; in the preparation of the manuscript; or in the review or approval of the manuscript.

CRediT authorship contribution statement

Sung-Hye You: Writing – original draft, Methodology, Investigation, Funding acquisition, Formal analysis, Data curation, Conceptualization. **Byungjun Kim:** Writing – review & editing, Methodology, Investigation, Funding acquisition, Data curation, Conceptualization. **Moonjung Hwang:** Writing – review & editing, Investigation, Formal analysis, Data curation. **Kyung-Sook Yang:** Methodology, Formal analysis. **Hye-Won Park:** Writing – review & editing, Formal analysis, Data curation. **InSeong Kim:** Software. **SuGil Kim:** Software. **Kyung Min Kim:** Investigation. **Bo Kyu Kim:** Writing – review & editing, Data curation. **Jae Ho Shin:** Writing – review & editing, Data curation.

Declaration of competing interest

The authors declare that they have no known competing financial interests or personal relationships that could have appeared to influence the work reported in this paper.

Acknowledgements

None.

Supplementary materials

Supplementary material associated with this article can be found, in the online version, at doi:10.1016/j.tjpad.2025.100323.

References

[1] De la Torre J. Impaired brain microcirculation may trigger Alzheimer's disease. Neurosci Biobehav Rev 1994;18:397–401.
[2] Knopman D. Cerebrovascular disease and dementia. Br J Radiol 2007;80:S121–7.
[3] Roher AE, Esh C, Rahman A, Kokjohn TA, Beach TG. Atherosclerosis of cerebral arteries in Alzheimer disease. Stroke 2004;35:2623–7.
[4] Tormos A, Taléns Visconti R, Pérez Garrido S, Rius Pérez S. Vascular pathology: cause or effect in Alzheimer disease? 2018.
[5] Pahlavian SH, Wang X, Ma S, et al. Cerebroarterial pulsatility and resistivity indices are associated with cognitive impairment and white matter hyperintensity in elderly subjects: A phase-contrast MRI study. J Cereb Blood Flow Metab 2021;41:670–83.
[6] Wymer DT, Patel KP, Burke III WF, VK Bhatia. Phase-contrast MRI: physics, techniques, and clinical applications. Radiographics 2020;40:122–40.
[7] Huang P, Chen K, Liu C, Zhen Z, Zhang R. Visualizing cerebral small vessel degeneration during aging and diseases using magnetic resonance imaging. J Magn Reson Imaging 2023;58:1323–37.
[8] Tomek A, Urbanová B, Hort J. Utility of transcranial ultrasound in predicting Alzheimer's disease risk. J Alzheimers Dis 2014;42:S365–74.
[9] Chung C-P, Lee H-Y, Lin P-C, Wang P-N. Cerebral artery pulsatility is associated with cognitive impairment and predicts dementia in individuals with subjective memory decline or mild cognitive impairment. J Alzheimers Dis 2017;60:625–32.

[10] Lim J-S, Lee JY, Kwon H-M, Lee Y-S. The correlation between cerebral arterial pulsatility and cognitive dysfunction in Alzheimer's disease patients. J Neurol Sci 2017;373:285–8.
[11] Nedergaard M, Goldman SA. Glymphatic failure as a final common pathway to dementia. Science (1979) 2020;370:50–6.
[12] Kiviniemi V, Wang X, Korhonen V, et al. Ultra-fast magnetic resonance encephalography of physiological brain activity–glymphatic pulsation mechanisms? J Cereb Blood Flow Metab 2016;36:1033–45.
[13] Taoka T, Ito R, Nakamichi R, Nakane T, Kawai H, Naganawa S. Diffusion tensor image analysis along the perivascular space (DTI-ALPS): revisiting the meaning and significance of the method. Magn Reson Med Sci 2024;23:268–90.
[14] Naganawa S, Taoka T, Ito R, Kawamura M. The glymphatic system in humans: investigations with magnetic resonance imaging. Invest Radiol 2024;59:1–12.
[15] Choi JD, Moon Y, Kim H-J, Yim Y, Lee S, Moon W-J. Choroid plexus volume and permeability at brain MRI within the Alzheimer disease clinical spectrum. Radiology 2022;304:635–45.
[16] Morgan CA, Thomas DL, Shao X, et al. Measurement of blood–brain barrier water exchange rate using diffusion-prepared and multi-echo arterial spin labelling: comparison of quantitative values and age dependence. NMR Biomed 2024;37:e5256.
[17] Kim J-H, Yoo R-E, Choi SH, Park S-H. Non-invasive flow mapping of parasagittal meningeal lymphatics using 2D interslice flow saturation MRI. Fluids Barriers CNS 2023;20:37.
[18] Webb AJ, Simoni M, Mazzucco S, Kuker W, Schulz U, Rothwell PM. Increased cerebral arterial pulsatility in patients with leukoaraiosis: arterial stiffness enhances transmission of aortic pulsatility. Stroke 2012;43:2631–6.
[19] Van Den Brink H, Doubal FN, Duering M. Advanced MRI in cerebral small vessel disease. Int J Stroke 2023;18:28–35.
[20] Arts T, Siero JC, Biessels GJ, Zwanenburg JJ. Automated assessment of cerebral arterial perforator function on 7T MRI. J Magn Reson Imaging 2021;53:234–41.
[21] Geurts LJ, Zwanenburg JJ, Klijn CJ, Luijten PR, Biessels GJ. Higher pulsatility in cerebral perforating arteries in patients with small vessel disease related stroke, a 7T MRI study. Stroke 2019;50:62–8.
[22] van den Kerkhof M, van der Thiel MM, van Oostenbrugge RJ, et al. Impaired damping of cerebral blood flow velocity pulsatility is associated with the number of perivascular spaces as measured with 7T MRI. J Cereb Blood Flow Metab 2023;43:937–46.
[23] Zong X, Lin W. Quantitative phase contrast MRI of penetrating arteries in centrum semiovale at 7T. Neuroimage 2019;195:463–74.
[24] Perosa V, Arts T, Assmann A, et al. Pulsatility index in the basal ganglia arteries increases with age in elderly with and without cerebral small vessel disease. Am J Neuroradiol 2022;43:540–6.
[25] Onkenhout L, Arts T, Ferro D, et al. Perforating artery flow velocity and pulsatility in patients with carotid occlusive disease. A 7 tesla MRI study. Cereb Circ - Cogn Behav 2022;3:100143.
[26] Arts T, Onkenhout LP, Amier RP, et al. Non-invasive assessment of damping of blood flow velocity pulsatility in cerebral arteries with MRI. J Magn Reson Imaging 2022;55:1785–94.
[27] van den Kerkhof M, van der Thiel MM, Postma AA, et al. Hypertension correlates with stronger blood flow pulsatility in small perforating cerebral arteries assessed with 7 tesla magnetic resonance imaging. Hypertension 2023;80:802–10.
[28] van den Kerkhof M, Jansen JF, van Oostenbrugge RJ, Backes WH. 1D versus 3D blood flow velocity and pulsatility measurements of lenticulostriate arteries at 7T MRI. Magn Reson Imaging 2023;96:144–50.
[29] Arts T, Meijs TA, Grotenhuis H, et al. Velocity and pulsatility measures in the perforating arteries of the basal ganglia at 3T MRI in reference to 7T MRI. Front Neurosci 2021;15:665480.
[30] van Tuijl RJ, Pham SD, Ruigrok YM, Biessels GJ, Velthuis BK, Zwanenburg JJ. Reliability of velocity pulsatility in small vessels on 3tesla mri in the basal ganglia: A test–retest study. Magnetic resonance materials in physics. Biol Med 2023;36:15–23.
[31] McKhann GM, Knopman DS, Chertkow H, et al. The diagnosis of dementia due to Alzheimer's disease: recommendations from the National Institute on Aging-Alzheimer's Association workgroups on diagnostic guidelines for Alzheimer's disease. Alzheimer's & dementia 2011;7:263–9.
[32] Shi Y, Thrippleton MJ, Marshall I, Wardlaw JM. Intracranial pulsatility in patients with cerebral small vessel disease: a systematic review. Clin Sci 2018;132:157–71.
[33] Wåhlin A, Eklund A, Malm J. 4D flow MRI hemodynamic biomarkers for cerebrovascular diseases. J Intern Med 2022;291:115–27.
[34] Roberts GS, Peret A, Jonaitis EM, et al. Normative cerebral hemodynamics in middle-aged and older adults using 4D flow MRI: initial analysis of vascular aging. Radiology 2023;307:e222685.